

1 Article

2 Cogging torque reduction based on a new pre-slot 3 technique for a small wind generator

4 Miguel García-Gracia ^{1*}, Ángel Jiménez Romero ¹, Jorge Herrero Ciudad² and Susana Martín
5 Arroyo¹

6 ¹ Dpto. Ingeniería Eléctrica, Universidad de Zaragoza; mggracia@unizar.es

7 ² For Optimal Renewable Energy Systems, S.L. (4fores); herrero@4fores.es

8 * Correspondence: mggracia@unizar.es; Tel.: +34-976-761923

9

10 **Abstract:** Cogging torque is a pulsating, parasitic and undesired torque ripple intrinsic of the
11 design of a permanent magnet synchronous generator (PMSG), which should be minimized due to
12 its adverse effects: vibration and noise. In addition, as aerodynamic power is low during start-up at
13 low wind speeds in small wind energy systems, the cogging torque must be as low as possible to
14 achieve a low cut-in speed. A novel mitigation technique using compound pre-slotting, based on a
15 combination of magnetic and non-magnetic materials, is investigated. The finite element technique
16 is used to calculate the cogging torque of a real PMSG design for a small wind turbine, with and
17 without using compound pre-slotting. The results show that cogging torque can be reduced by a
18 factor of 48% with this technique, while avoiding the main drawback of the conventional
19 pre-slotting technique: the reduction of induced voltage due to leakage flux between stator teeth.
20 Furthermore, through a combination of pre-slotting and other cogging torque optimization
21 techniques, 84%, cogging torque can be eliminated for a given design.

22

23 **Keywords:** cogging torque; permanent magnet synchronous generator; small wind turbines; finite
24 element method; renewable energy, energy conversion.

25

26 1. Introduction

27 Increasing interest in the efficiency of electric machinery and reducing maintenance costs is
28 making the use of permanent magnet synchronous generators (PMSGs) more common. PMSGs
29 combine high efficiency with low maintenance and a high power density [1], factors that make them
30 extremely attractive for use in renewable energy applications, such as wind [2], wave power [3] and
31 tidal power [4], or electrical mobility applications [5] and, in general, in uses where they must act as
32 a motor or generator. Furthermore, in renewable energy applications, PMSGs allow direct-drive
33 configurations, making the use of gearbox unnecessary or reducing the number of gearbox stages,
34 which decreases the overall generator volume and improves its efficiency [6].

35 However, machines based on permanent magnets (PMs) also have some drawbacks, and the
36 cogging torque is one of the main ones. The magnetic interaction between the flux generated by the
37 rotor PMs and the stator geometry results in a pulsating torque called cogging torque, which,
38 depending on the PM machine design, can cause an undesired ripple in both the machine's induced
39 voltage (EMF) and its mechanical torque [7,8]. Other problems with PMSGs are the vibrations and
40 noise they make. Since this type of machine has high magnetic flux density values in the air gap, the
41 electromagnetic forces between the PMs and the stator teeth are high [9]. These electromagnetic
42 forces are divided into two components, one radial and the other tangential. The tangential

43 component of the electromagnetic force contributes to the torque in the stator teeth, while the radial
44 component causes vibrations and even deformations in the machine [10]. These radial forces act on
45 the stator producing vibrations and noise, especially when their frequency coincides with the
46 natural frequency of the machine's mechanical structure [11].

47 The cogging torque is especially important in wind energy applications as it establishes in which
48 conditions the system will begin generating. The mechanical torque captured by the generation
49 system must be larger than the cogging torque starting the rotation, which is why achieving a
50 reduced cogging torque is one of the objectives for this type of machine.

51 There are several methods to reduce cogging torque in the PMSG design phase. The most used
52 is skewing, which consists of preventing the stator teeth and the magnets from becoming aligned by
53 either turning the stator teeth [6, 12] or the rotor's permanent magnets [1, 2, 13]. The required skew
54 angle to largely cancel out the effect of the interactions between the PMs and the slots depends on
55 how many slots and poles the machine has. Other methods study the use of notches in stator teeth
56 [7, 14]. These notches produce the same effect in the magnetic interaction as the slots and increase
57 the effective number of slots, which impacts on the cogging torque as it depends on how many poles
58 and slots the machine has. Therefore, this method's effectiveness is conditioned by the number of
59 poles and slots selected in the design.

60 A study is presented in [15, 16] in which slot openings in one half of the stator shift in one
61 direction with respect to the tooth and the other half shift in the other direction. This means the
62 cogging torque waveform moves in opposite directions in each machine half and the cogging caused
63 by each machine half may be cancelled out depending on the shifted angle. Other studies focus on
64 the shape of PM edges, concluding that their size can be reduced on the magnet sides to lessen air
65 gap reluctance variation, which reduces the magnetic energy variation in the machine and,
66 therefore, mitigates the cogging torque [17, 18].

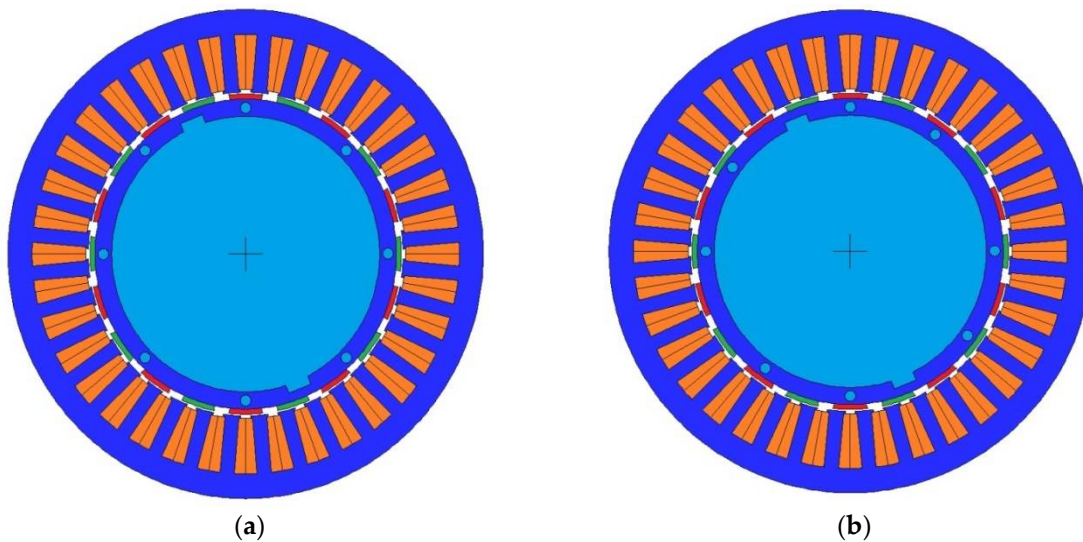
67 Several authors have conducted studies of PMSG with closed slots and their effects. Leakage
68 fluxes caused as a result of closing stator slots are analyzed in [4], concluding that the size of PMs
69 should be increased to compensate flux loss through closed slots. The increase in iron losses caused
70 by tooth-tip saturation, distortion in the induced voltage this saturation causes and how the use of
71 closed slots influences this are studied in [19 and 20]. The study by [21] focuses on average torque
72 and its ripple in machines with closed slots for several stator types.

73 Unlike the above-mentioned methods, which focus on minimizing the cogging torque in the
74 machine design stage, this article proposes a cogging torque reduction method that is easy to
75 implement without the need for any changes to the original design of the machine, a 6.3-kW
76 generator for a small wind turbine. The suggested solution comprises sliding a metal part (pre-slot)
77 into the slots after completing the machine winding. This technique minimizes slot openings so that
78 induced voltage remains unaltered and the mounting of machine windings is not hampered. The
79 results of the proposed method are analyzed using FEMM 2D finite element software on an original
80 PMSG design and compared with the results obtained experimentally. Additionally, constructive
81 improvements are suggested to reduce cogging torque. Finally, the article shows how the proposed
82 technique can also be combined with the skewing technique, thus significantly reducing the cogging
83 torque to 0.03 Nm in the ideal case and 0.51 Nm when imperfections in the manufacturing process
84 are considered.

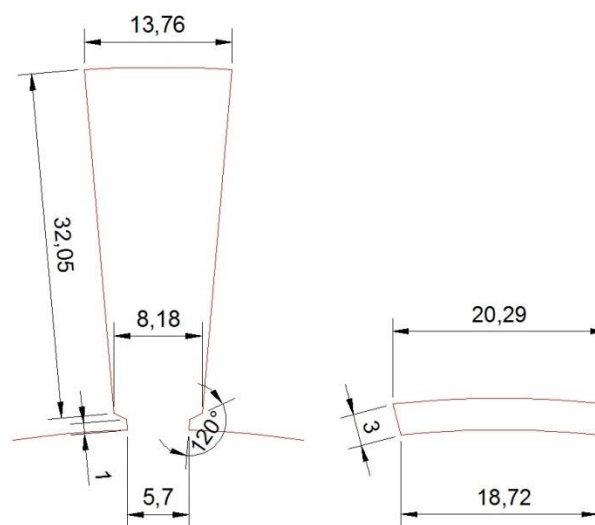
85 2. Machine type and main parameters

86 The machine involved in this study is a 6.3 kW PMSG with an interior rotor and
 87 surface-mounted magnets comprising 36 slots and 20 poles. Figure 1(a) is a cross section of the
 88 generator showing the slots forming the stator, the rotor in the internal part and the
 89 surface-mounted magnets above it in the central part. The details of the millimeter measurements of
 90 the machine's slots and PMs are shown in Figure 2. The characteristic parameters of the studied
 91 PMSG are shown in Table 1.

92 The analysis of the PMSG and the cogging torque reduction methods proposed in this study has
 93 been performed using FEMM 2D finite element software. To validate the FEMM model used in the
 94 cogging torque reduction analysis a comparison will be made with the experimental values of the
 95 original machine.
 96



97 **Figure 1.** Cross section area of the PMSG: (a) Original model; (b) Model with centered holes.



98
 99 **Figure 2.** Slot and magnet dimensions (mm).

100 **Table 1.** Parameters of the PMSG machine.

Parameter	Value
Phase	3
Pole number	20
Slot number	36
Rated speed	232 rpm
Rated power	6300 W
Rated voltage	256.4 V
Air gap	1 mm
Thickness of PM	3 mm
Air gap diameter	188 mm
Material of steel	M330-50A
Material of PM	NdFeB

101 3. Cogging torque

102 Cogging torque is a parasitic torque resulting from interactions between the rotor's permanent
 103 magnets and the stator slots. Air gap reluctance differs depending on the rotor's angular position to
 104 the slots. Rotor magnets tend to align with the stator in the position in which air gap permeance is
 105 larger [22], so when they are shifted from this position during rotation, they generate a torque, the
 106 cogging torque.

107 Electromagnetic torque can be obtained from the variation in the total energy of the magnetic
 108 field compared with the angular position of the rotor θ when excitation current is constant [14]

$$T = -\frac{\partial W_c}{\partial \theta} \quad (1)$$

109 The total energy stored in the magnetic field or coenergy W_c in a PMSG is given by [7]

$$W_c = \frac{1}{2} L i^2 + \frac{1}{2} (R + R_m) \Phi_m^2 + N i \Phi_m \quad (2)$$

110 where L is the inductance of the windings, i the excitation current, R and R_m are, respectively, the
 111 reluctances viewed by the magnetomotive force and by the magnetic field, Φ_m the flux due to the
 112 magnets crossing the air gap, and N the number of winding turns.

113 Therefore, substituting in (2) results in

$$T = \frac{1}{2} i^2 \frac{dL}{d\theta} - \frac{1}{2} \Phi_m^2 \frac{dR}{d\theta} + N i \frac{d\Phi_m}{d\theta} \quad (3)$$

114 The second term of (3) corresponds to magnet reluctance torque and it is known as cogging
 115 torque [17], T_{cog} .

$$T_{cog} = -\frac{1}{2} \Phi_m^2 \frac{dR}{d\theta} \quad (4)$$

116 As observed in (4), cogging torque is independent of the current and corresponds to the result
 117 of analyzing (3) when the machine is in open circuit. Cogging torque depends on magnetic flux and
 118 on the rate of change of air-gap reluctance. From (4), to minimize T_{cog} , reluctance R should be
 119 independent of the rotor position. Therefore, a very low cogging torque design requires an almost
 120 constant value of R for any rotor position.

121

122

123 4. Cogging torque measurement

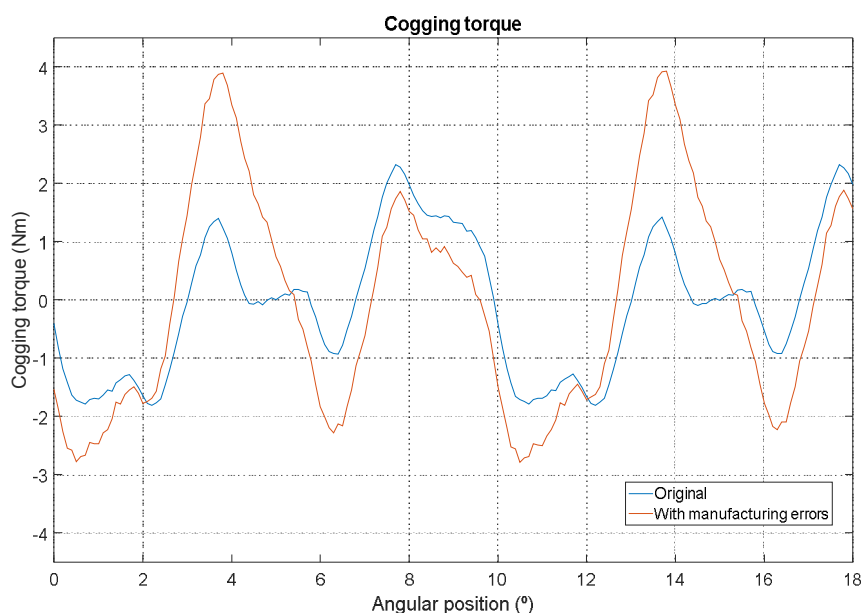
124 Cogging torque is calculated in FEMM for every angular rotor position, making the machine
 125 operate off-load. The torque is calculated by integrating the Maxwell stress tensor throughout the air
 126 gap

$$T_{cog} = \frac{L}{g \mu_0} \int_S r B_n B_t dS \quad (5)$$

127 where L is the rotor depth, g is the air gap length, B_n the normal flux density, B_t the tangential flux
 128 density and r the radius from the center of the rotor to the center of the air gap [7].

129 Compared with the results obtained when the calculation is based on the magnetic energy
 130 variation with respect to the angular rotor position given by (1), in [18] it is shown that both methods
 131 obtain almost identical results.

132 The simulation in FEMM of the PMSG in Figure 1 (a) obtained the cogging torque shown in
 133 Figure 3 (“original” curve), whose maximum value is 2.32 Nm, while the experimental results of the
 134 machine show maximum values of 3.70 Nm. The main reason for this deviation from experimental
 135 values is due to component manufacturing tolerance. Consequently, if a tolerance of ± 0.1 mm is
 136 included in the 20 PMs of the PMSG model and this error is distributed randomly at the height of the
 137 PMs, the result shown in Figure 3 (curve “with manufacturing errors”) is obtained. Having magnets
 138 that are not the same impacts the cogging torque significantly, mainly because differently sized PMs
 139 cause higher magnetic flux variations in the air gap. The maximum cogging torque value obtained in
 140 the simulation is 3.90 Nm (Figure 3). This value is slightly higher than the experimental PMSG
 141 results, making it possible to validate the developed FEMM model with respect to the cogging
 142 torque analysis.



143

144 **Figure 3.** Simulation results of cogging torque of the original model considering manufacturing errors.

145

146

147

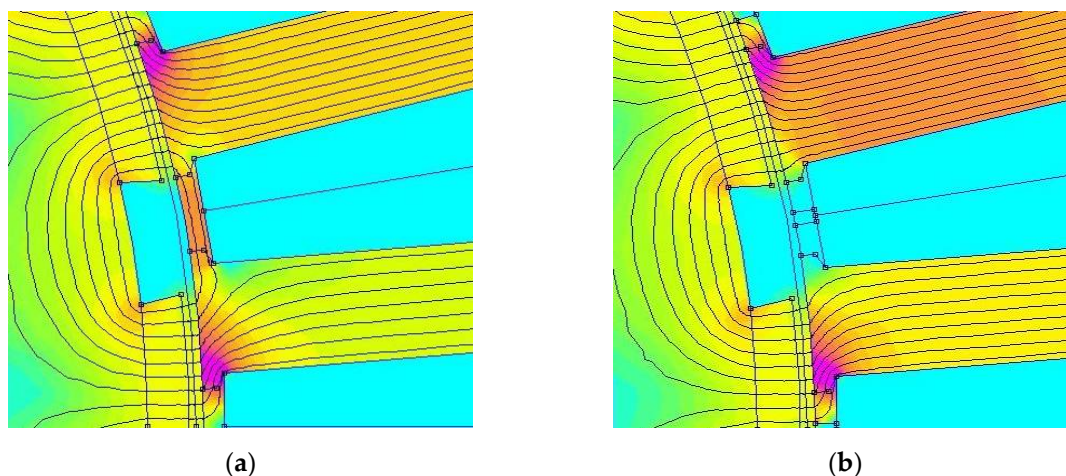
148 5. Cogging torque reduction methods

149 5.1. Pre-slot method

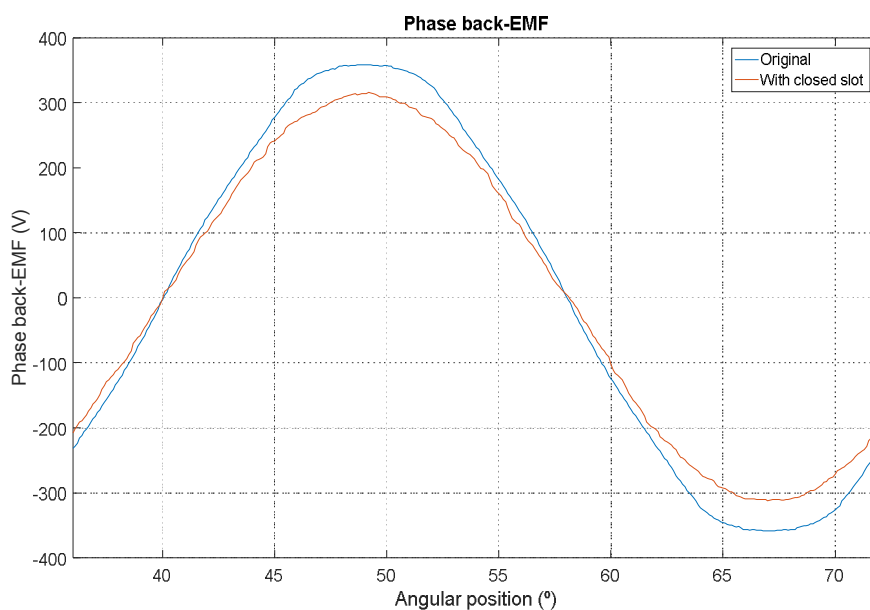
150 The main objective is to reduce the cogging torque without affecting the machine's construction
151 characteristics and, therefore, without making any changes in the generator's geometry.

152 A closed-slot stator topology reduces reluctance variation in the air gap and, therefore, the
153 machine's maximum cogging torque value. Furthermore, the minimum dimensions of PMSG slot
154 openings are conditioned by winding mounting factors. Their minimum size depends on the cross
155 section of the winding conductors so that they can be inserted in the slot.

156 Furthermore, the slot closing method has the drawback of generating a leakage flux through the
157 slots due to the high permeability of the magnetic core connecting the teeth, Figure 4 (a). These
158 leakages reduce the flux linked by the machine windings, thus producing a drop in induced voltage.
159 This drop in induced voltage can be seen in Figure 5, showing the induced voltage of the PMSG with
160 open slots (the "original" curve) and with closed slots. The effective induced voltage value is 256.4 V
161 in the original generator model with open slots, and it decreases to 221.6 V when the slots are closed.



162 **Figure 4.** Magnetic field lines ($\theta=0^\circ$): (a) Model with closed slots; (b) Model with pre-slots.



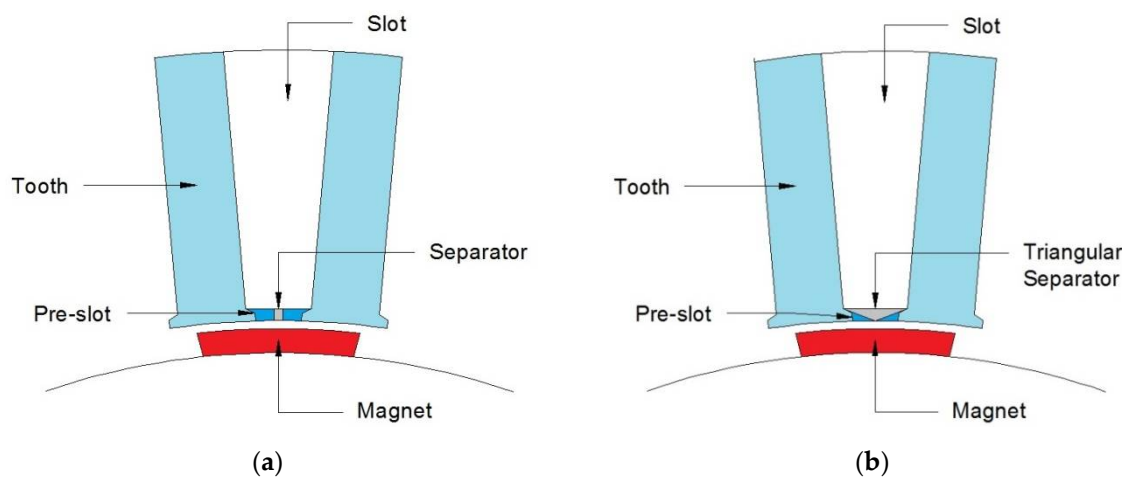
163

164

Figure 5. Effect of closed slots in back electromotive force (EMF).

165 To avoid the above-mentioned drawbacks, the proposed cogging torque reduction method
 166 consists of closing the slots by sliding in a pre-slot part made of the same ferromagnetic material as
 167 the stator, as observed in Figure 6. The pre-slot is placed between the teeth longitudinally after
 168 machine winding; this does not alter the winding or the slot fill factor. Figure 6 (a) provides details of
 169 the space between two of the machine's stator teeth showing where the ferromagnetic part is slid
 170 into the start of each slot. The pre-slot considered in this study is 1.5 mm high; its dimensions are
 171 adjusted to the available space to render changing the machine winding unnecessary.

172 A material separator with low magnetic permeability (aluminum or similar) and a width of
 173 1 mm, the same distance as the machine's air gap, is in the central part of the pre-slot. The purpose of
 174 the central separator is to prevent the above-mentioned flux leakage linked by the windings. As this
 175 is a non-magnetic separator, it prevents the pre-slot from closing the magnetic field lines and,
 176 therefore, preventing flux from circulating between two consecutive PMs.

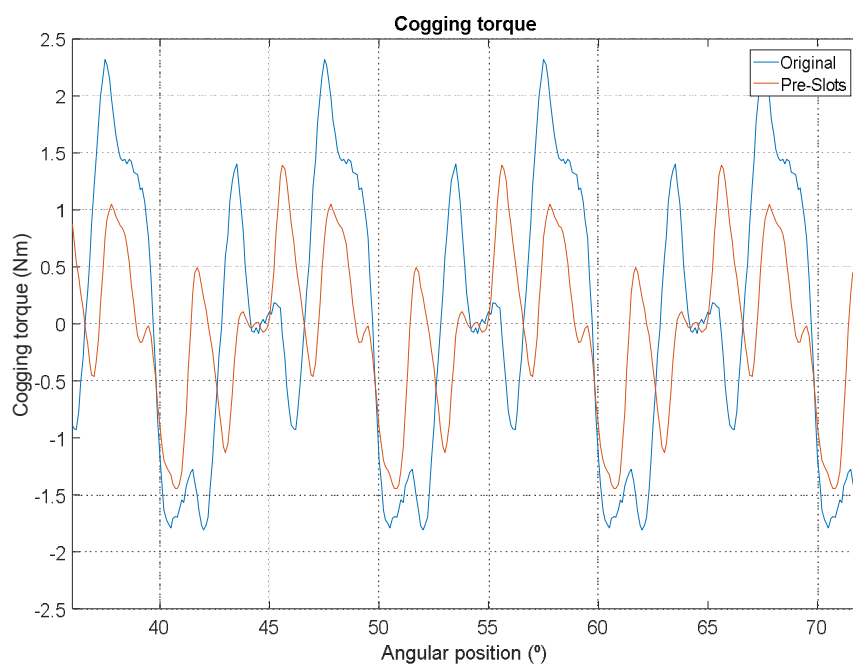


177 **Figure 6.** Proposed cogging-torque reduction method: (a) Pre-slot with separator; (b) Pre-slot with triangular
 178 separator.

179 In accordance with the developed FEMM model, inserting pre-slots with a separator manages
 180 to reduce the maximum cogging torque value by 37.9% compared with the original PMSG, as
 181 observed in the results shown in the graph in Figure 7, but it does not decrease induced voltage as
 182 using the separator reduces leakages.

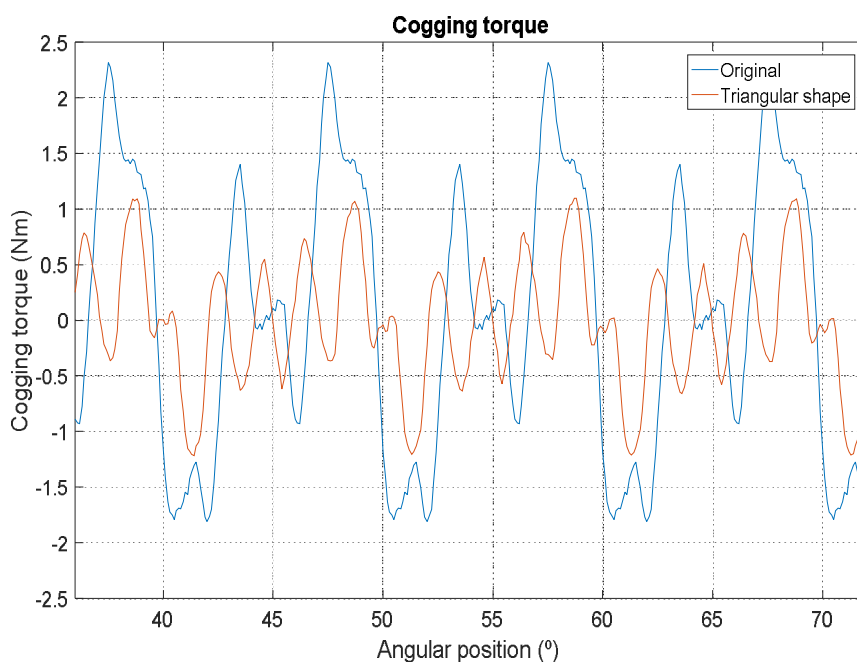
183 This cogging torque reduction can be improved by considering other alternative geometrical
 184 pre-slot configurations. A triangular separator, as shown in Figure 6 (b), can lessen the magnetic
 185 energy variation caused in the original teeth edges or in pre-slot separators, which decreases the
 186 machine's cogging torque.

187 Pre-slot geometry with a triangular separator prevents leakage flux through it, as occurs with
 188 the central separator model, thus preventing the undesired decrease in induced voltage and in
 189 linked flux through machine windings. Similarly, it produces a higher reduction in maximum
 190 cogging torque, as shown in the graph in Figure 8, decreasing the cogging torque generated by over
 191 47.8%.



192
193

Figure 7. Comparison of cogging torque reduction with pre-slot method.

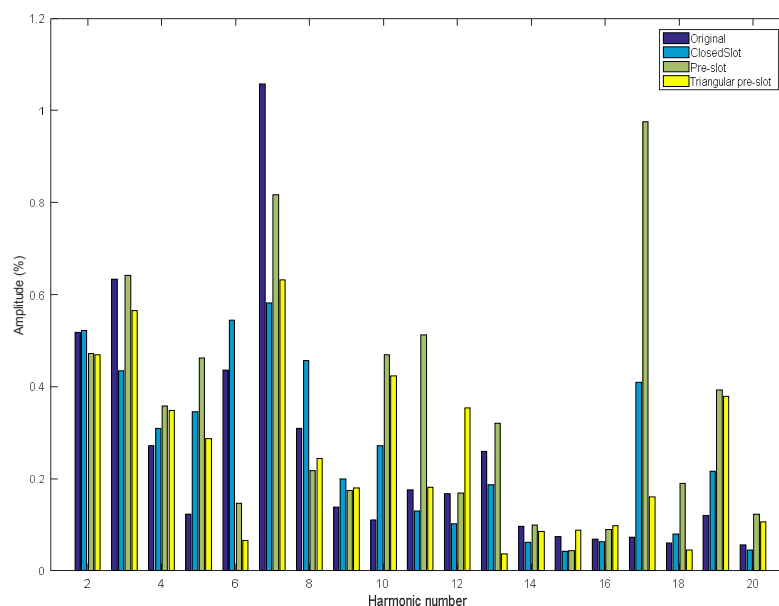


194
195

Figure 8. Comparison of cogging torque reduction with the triangular pre-slot method.

196 An analysis of induced voltage harmonics was conducted to confirm that the installation of the
 197 proposed pre-slot system to reduce cogging torque does not affect the machine's technical
 198 characteristics. The PMSG is designed for small wind-power applications and, therefore, if an
 199 uncontrolled rectifier is used, the harmonics level is of no importance. However, if the connection is
 200 via a full converter, the opposite is the case. Figure 9 shows the frequency spectrum of the first 20
 201 harmonics of each of the waves and the harmonic distortion rate (THD) for each model; therefore,
 202 the analysis was conducted from the fundamental frequency of 38.67 Hz to the twentieth harmonic
 203 (773.4 Hz).

204 Table 2 shows how the THD values obtained remain low and similar across all cases and never
 205 exceed 2%. The pre-slot solution with a triangular separator presents the least harmonic distortion of
 206 the considered models; it is very similar to the closed-slot model and improves the original
 207 configuration.



208
 209 **Figure 9.** Harmonic spectrum for the proposed reduction method.

210 **Table 2.** THD of the different models.

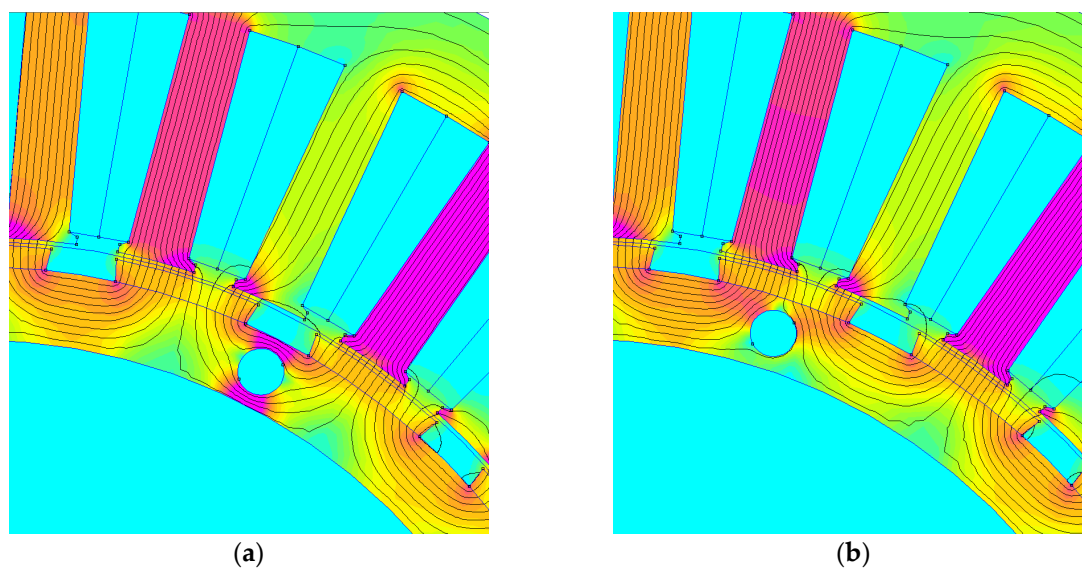
Model	THD (%)
Original design	1.54
Design with closed slot	1.39
Design with pre-slot	1.88
Design with triangular pre-slot	1.33

211

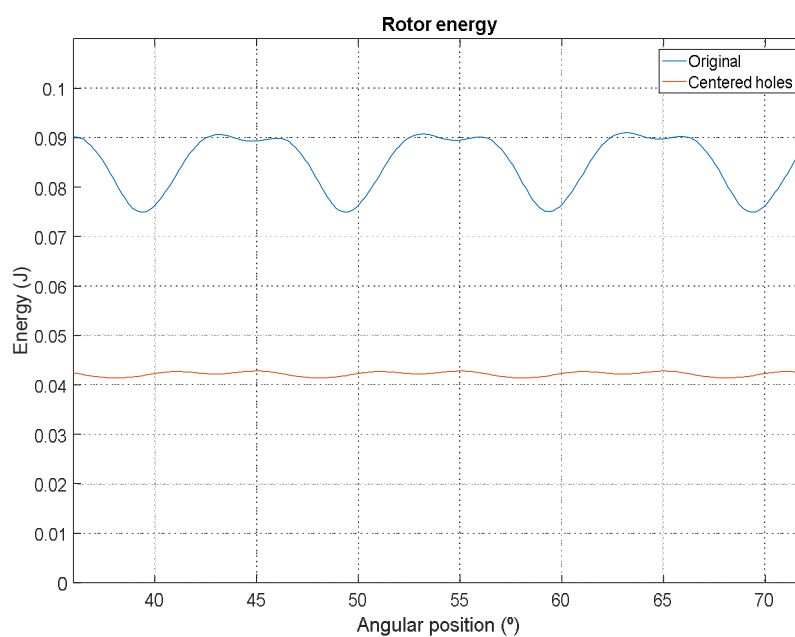
212 5.2. Manufacturing aspects to reduce the cogging torque

213 Any change in the magnetic circuit alters its reluctance and, therefore, in accordance with (4), it
 214 affects the cogging torque and must be considered to reduce it. Consequently, it was found that the
 215 holes for correctly aligning the rotor sheet metal with screws in the original design significantly
 216 influence the machine's cogging torque, depending on their position with respect to the PMs, Figure
 217 1(b).

218 The impact of these holes on the cogging torque was analyzed for their different positions with
 219 respect to the PMs. The conclusion is that the optimal position, which minimizes cogging torque, is a
 220 centered position with respect to the magnets. Figure 10 (b) shows the case in which the rotor hole is
 221 centered with respect to the PMs. In this situation, the holes have virtually no influence on magnetic
 222 field lines linking one magnet with another. In contrast, when the hole is decentered, Figure 10 (a),
 223 the effect is a smaller effective area in the rotor through which the field lines circulate. Therefore,
 224 reluctance increases with respect to the case shown in Figure 10 (b) (centered hole) and the magnetic
 225 energy in the rotor decreases as observed in Figure 11.

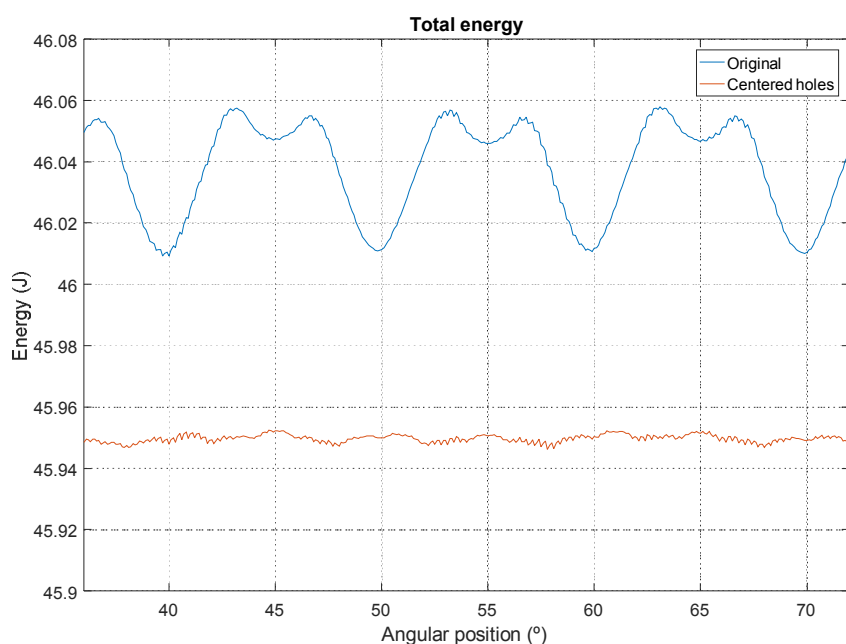


226 **Figure 10.** Magnetic field distribution ($\theta=0^\circ$): (a) Original model, without centered holes; (b) Model with
 227 centered holes.



228 **Figure 11.** Magnetic energy in the rotor.
 229

230 Figure 12 shows the magnetic energy stored in the machine with respect to the rotor during
 231 electrical 360° (mechanical 36°) for both PMSG models. If the hole is decentered, energy minimums
 232 occur when the hole is aligned with a stator tooth. In this position, the flux between two adjacent
 233 magnets would be the maximum if there was no hole. Consequently, as observed in Figure 12, and
 234 given that the teeth are distributed every mechanical 10° along the stator, the energy minimum
 235 occurs with this frequency.



236

237

Figure 12. Total magnetic energy.

238

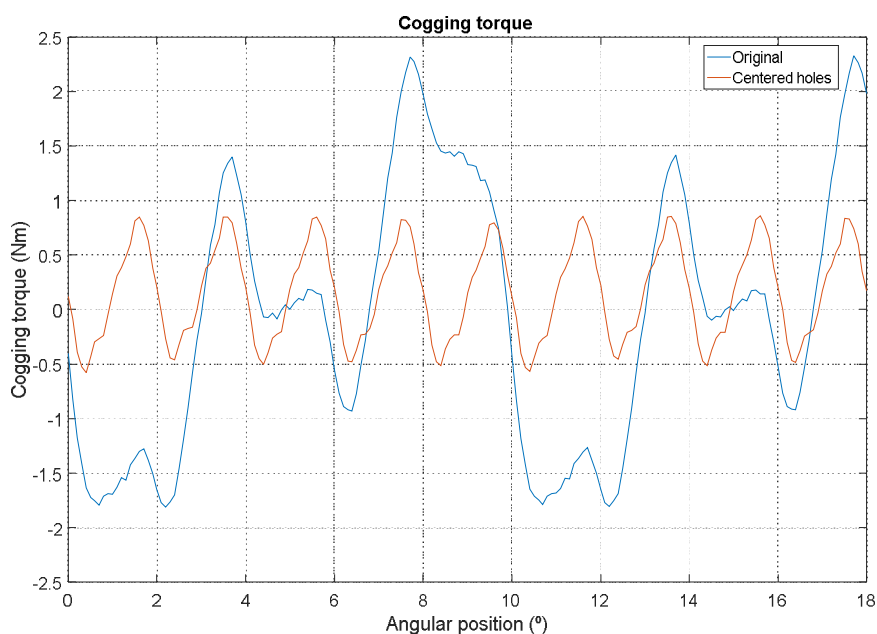
239

240

241

242

Figure 13 compares the cogging torque for both PMSGs, resulting in a higher value when the hole is decentered given that more magnetic energy variations occur, as presented in Figure 12. The cogging torque of the model with decentered holes is 2.32 Nm, while this value does not exceed 0.86 Nm when the holes are centered. Figure 13 also shows that the presence of decentered holes even produces a change in the cogging torque wave period.



243

244

Figure 13. Cogging torque of the original PMSG and model with centered holes.

245

246

247

248 5.3. Comparative results

249 Table 3 compares the maximum cogging torque values obtained with the original design with
 250 the two proposed pre-slot configurations and shows the reduction percentage with respect to the
 251 original design. The results of the different models are shown in the ideal case (with no
 252 manufacturing errors) and considering manufacturing errors in the magnets.

253
 254 **Table 3.** Comparison of the maximum cogging torque values obtained for the prototype and the different
 255 models considered in the study.

Model	Without manufacturing errors		Considering manufacturing errors	
	Nm	Reduction (%)	Nm	Reduction (%)
Original design (without centered holes)				
Prototype	3.70			
Original design	2.32	-	3.92	-
Pre-slot with separation	1.44	37.9	2.03	48.2
Triangular pre-slot	1.21	47.8	1.90	51.5
Design with all holes centered				
Original design	0.86	-	3.31	-
Pre-slot with separation	0.61	29.1	1.80	45.6
Triangular pre-slot	0.59	31.4	1.76	46.8

256

257 Finally, the proposed pre-slot method was compared with the skewing technique and the
 258 combination of both is considered. The technique of fractional skewing in the rotor [23] comprises
 259 dividing the rotor and turning one division away from another for half the cogging torque period.
 260 Four divisions have been considered in this analysis, as observed in Figure 14. Therefore,
 261 considering that the cogging torque period is mechanical 2° , the shift of one division with respect to
 262 another is half of this period, which equals 1° . As observed in Table 4, concerning the model with
 263 centered holes and in the ideal case of having no manufacturing errors, applying this combined
 264 technique manages to reduce the cogging torque to a peak value of 0.03 Nm or to 0.51 Nm if
 265 manufacturing errors are considered. In either of the two cases, the cogging torque reduction is very
 266 significant.

267 Figure 15 shows the cogging torque waveform obtained for the PMSG with centered holes.
 268 Because of the reluctance periodicity, the cogging torque is a periodic waveform with a frequency
 269 given by:

$$f_{T_{cog}} = \frac{\omega \cdot LCM(N_{slots}, N_{poles})}{360^\circ} = 696 \text{ Hz} \quad (6)$$

270 where ω is the mechanical speed (1392°/s), LCM the least common multiple of the number of slots
 271 ($N_{slots}=36$) and the number of poles ($N_{poles}=20$). The results in Figure 15 show the decrease in the
 272 cogging torque with the pre-slot triangular method and that this improvement is even better when
 273 combining this pre-slot installation technique with fractional skewing in the rotor, up to 84% less in
 274 the most realistic case of considering errors in manufacturing processes.

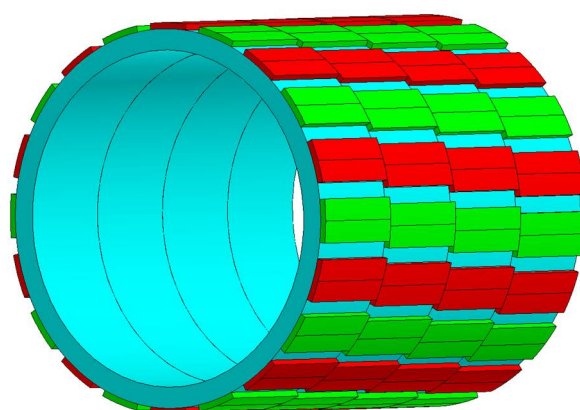


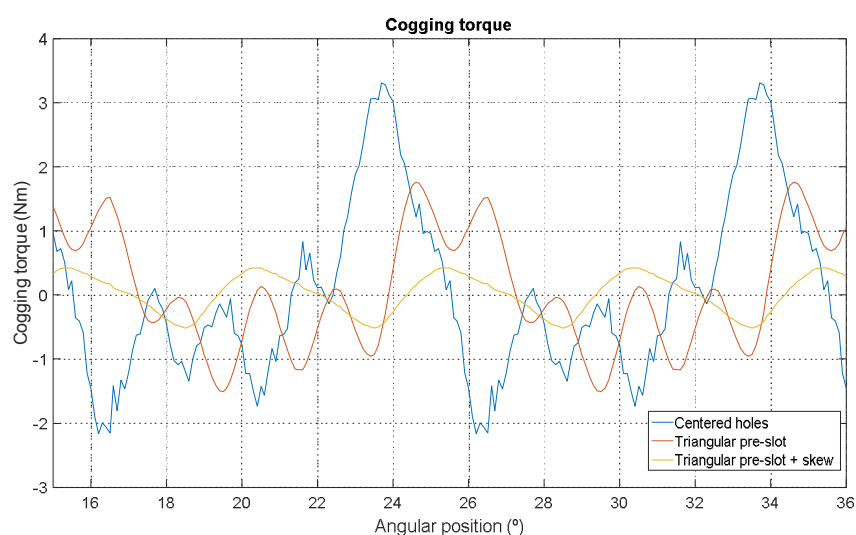
Figure 14. Fractional skewing in the rotor.

275

276

277 **Table 4.** Comparison of the maximum cogging torque values of PMSG with centered holes and the different
278 models considering skewing.

Model	Without manufacturing errors		Considering manufacturing errors	
	Nm	Reduction (%)	Nm	Reduction (%)
Design with centered holes	0.86	-	3.31	-
Design with centered holes + Triangular pre-slot	0.59	31.4	1.76	46.8
Design with centered holes + Skewing	0.31	64.0	1.34	59.5
Design with centered holes + Triangular pre-slot + Skewing	0.03	96.5	0.51	84.6



279

280 **Figure 15.** Cogging torque of the centered holes PMSG model, triangular pre-slot model and triangular pre-slot
281 model with skewing (with manufacturing errors).

282

283

284

285 6. Conclusions

286 This article presents a new cogging torque reduction technique that does not require changes to
287 the machine's main geometry. It proposes placing pre-slots in the initial part of the stator slots. These
288 pre-slots are made of the same ferromagnetic material as the stator, with a non-magnetic central
289 separator (in two halves). The pre-slots are slid longitudinally between the slots after completing
290 machine winding and, therefore, without altering the PMSG's fill factor.

291 Introducing a central part of non-magnetic material prevents leakage flux between the
292 machine's teeth and also stops its induced voltage from reducing significantly with respect to the
293 configuration without pre-slots.

294 The proposed method manages to reduce cogging torque in PMSGs with surface-mounted
295 magnets by up to 47.8%. Additionally, the article analyzes how changing the magnetic circuits for
296 construction reasons can affect the cogging torque, which can easily be optimized. The pre-slot
297 technique is also compatible with other cogging torque reduction techniques, such as skewing.
298 When the above-mentioned methods are combined, cogging torque is reduced by 84.6% considering
299 manufacturing errors.

300

301 **Author Contributions:** Miguel García-Gracia and Ángel Jiménez Romero performed the simulations and wrote
302 the paper. 4fores contributed with the prototype and valuable comments and corrections. All authors discussed
303 the results and commented on the manuscript at all stages.

304 **Funding:** This research was funded by "Ministerio de Economía, Industria y Competitividad (Plan Estatal de
305 Investigación Científica y Técnica y de Innovación 2013-2016)" and "Fondo Europeo de Desarrollo Regional FEDER",
306 grant number RTC-2016-5234-3, in the frame of the Project MHiRED "Nuevas tecnologías para minirredes híbridas
307 eólica-fotovoltaica gestionadas con almacenamiento en conexión a red y con apoyo síncrono en funcionamiento en isla".

308 **Acknowledgments:** The authors wish to thank 4fores for granting their permission to publish some data
309 presented in this article. Furthermore, the technical support from the Research Group on Renewable Energy
310 Integration of the University of Zaragoza (funded by the Gobierno de Aragón) is also gratefully acknowledged.

311 **Conflicts of Interest:** The authors declare no conflict of interest.

312

313 References

- 314 1. Fei, W.; Zhu, Z. Q. Comparison of Cogging Torque Reduction in Permanent Magnet Brushless Machines
315 by Conventional and Herringbone Skewing Techniques. *IEEE Trans. Energy Convers.* **2013**, *28* (3), 664–674.
- 316 2. Ose-zala, B.; Pugachov, V. Methods to Reduce Cogging Torque of Permanent Magnet Synchronous
317 Generator Used In Wind Power Plants. *Elektron. ir Elektrotehnika* **2017**, *23* (1), 43–48.
- 318 3. Leijon, J.; Sjölund, J.; Ekergård, B.; Boström, C.; Eriksson, S.; Temiz, I.; Leijon, M. Study of an Altered
319 Magnetic Circuit of a Permanent Magnet Linear Generator for Wave Power. *Energies* **2018**, *11* (1), 1–13.
- 320 4. Lejerskog, E.; Leijon, M. Detailed Study of Closed Stator Slots for a Direct-Driven Synchronous Permanent
321 Magnet Linear Wave Energy Converter. *Machines* **2014**, *2* (1), 73–86.
- 322 5. Raihan, M. A. H.; Smith, K. J.; Almoraya, A. A.; Khan, F. Interior Permanent Magnet Synchronous Machine
323 (IPMSM) Design for Environment Friendly Hybrid Electric Vehicle (HEV) Applications. In *Humanitarian
324 Technology Conference (R10-HTC), 2017 IEEE Region 10; 2017; pp 21–23.*

- 325 6. Öztürk, N.; Dalcali, A.; Çelik, E.; Sakar, S. Cogging Torque Reduction by Optimal Design of PM
326 Synchronous Generator for Wind Turbines. *Int. J. Hydrogen Energy* **2017**, *42* (28), 17593–17600.
- 327 7. Ozoglu, Y. New Stator Tooth for Reducing Torque Ripple in Outer Rotor Permanent Magnet Machine.
328 *Adv. Electr. Comput. Eng.* **2016**, *16* (3), 49–56.
- 329 8. Liu, C.; Lu, J.; Wang, Y.; Lei, G.; Zhu, J.; Guo, Y. Techniques for Reduction of the Cogging Torque in Claw
330 Pole Machines with SMC Cores. *Energies* **2017**, *10* (10), 1–17.
- 331 9. Ito, T.; Akatsu, K. Electromagnetic Force Acquisition Distributed in Electric Motor to Reduce Vibration.
332 *IEEE Trans. Ind. Appl.* **2017**, *53* (2), 1001–1008.
- 333 10. Chen, Y. S.; Zhu, Z. Q.; Howe, D. Vibration of PM Brushless Machines Having a Fractional Number of
334 Slots per Pole. *IEEE Trans. Magn.* **2006**, *42* (10), 3395–3397.
- 335 11. Min, S. G.; Bramerdorfer, G.; Sarlioglu, B. Analytical Modeling and Optimization for Electromagnetic
336 Performances of Fractional-Slot PM Brushless Machines. *IEEE Trans. Ind. Electron.* **2017**, *65* (5), 4017–4027.
- 337 12. Tseng, W.; Chen, W. Design Parameters Optimization of a Permanent Magnet Synchronous Wind
338 Generator. *19th Int. Conf. Electr. Mach. Syst.* 2016.
- 339 13. Levin, N.; Orlova, S.; Pugachov, V.; Ose-Zala, B.; Jakobsons, E. Methods to Reduce the Cogging Torque in
340 Permanent Magnet Synchronous Machines. *Electron. Electr. Eng.* **2013**, *19* (1), 23–26.
- 341 14. Ma, G.; Li, G.; Zhou, R.; Guo, X.; Ju, L.; Xie, F. Effect of Stator and Rotor Notches on Cogging Torque of
342 Permanent Magnet Synchronous Motor. *IEEE Trans. Ind. Appl.* **2017**, No. 1.
- 343 15. Liu, T.; Huang, S.; Gao, J.; Lu, K. Cogging Torque Reduction by Slot-Opening Shift for Permanent Magnet
344 Machines. *IEEE Trans. Magn.* **2013**, *49* (7), 4028–4031.
- 345 16. Dajaku, G.; Gerling, D. New Methods for Reducing the Cogging Torque and Torque Ripples of PMSM.
346 *2014 4th Int. Electr. Drives Prod. Conf. EDPC 2014 - Proc.* 2014.
- 347 17. Hsiao, C.; Yeh, S.; Hwang, J. Permanent Magnet Structure Optimization for Cogging Torque Reduction of
348 Outer Rotor Type Radial Flux Permanent Magnet Generator. A novel cogging torque simulation method
349 for permanent-magnet synchronous machines. *Energies* **2011**, *4*, 2166–2179.
- 350 18. Imamori, S.; Ohguchi, H.; Shuto, M.; Toba, A. Relation between Magnetic Properties of Stator Core and
351 Cogging Torque in 8-Pole 12-Slot SPM Synchronous Motors. *IEEE J. Ind. Appl.* **2015**, *4* (6), 696–702.
- 352 19. Wu, D.; Zhu, Z. Q.; Chu, W. Q. Iron Loss in Surface-Mounted PM Machines Considering Tooth-Tip Local
353 Magnetic Saturation. *2016 IEEE Veh. Power Propuls. Conf. VPPC 2016 - Proc.* 2016, No. 2011.
- 354 20. Wu, D.; Zhu, Z. Q. On-Load Voltage Distortion in Fractional Slot Surface-Mounted Permanent Magnet
355 Machines Considering Local Magnetic Saturation. *IEEE Trans. Magn.* **2015**, *51* (8).
- 356 21. Li, Y. X.; Li, G. J. Influence of Stator Topologies on Average Torque and Torque Ripple of Fractional-Slot
357 SPM Machines with Fully Closed Slots. *IEEE Trans. Ind. Appl.* **2018**, 9994 (c), 1–1.

- 358 22. Todorov, G.; Stoev, B.; Savov, G.; Kyuchukov, P. Effects of Cogging Torque Reduction Techniques
359 Applied to Surface Mounted PMSMs with Distributed Windings. *2017 15th Int. Conf. Electr. Mach. Drives*
360 *Power Syst. ELMA 2017 - Proc.* 2017, 17–21.
- 361 23. Galfarsoro, U.; Parra, J.; McCloskey, A.; Zarate, S.; Hernandez, X. Analysis of Vibration Induced by
362 Cogging Torque in Permanent-Magnet Synchronous Motors. *Proc. 2017 IEEE Int. Work. Electron. Control.*
363 *Meas. Signals their Appl. to Mechatronics, ECMSM 2017* 2017.
- 364